Plasma deposited high density amines on surface using (3-aminopropyl)triethoxysilane for assembling particles at near-nano size

Xi Rao [a,b,c,*], Ali Abou Hassan [d], Cédric Guyon [b], Stephanie Ognier [b], Michaël Tatoulian [b,**]

[a] Key Laboratory of Luminescent and Real-Time Analytical Chemistry (Southwest University), Ministry of Education, School of Materials and Energy, Southwest University, Chongqing, 400715, PR China
[b] Chimie ParisTech, PSL University, CNRS, Institut de Recherche de Chimie Paris, 75005, Paris, France
[c] Chongqing Key Laboratory of Soft-Matter Material Chemistry and Function Manufacturing, Southwest University, Chongqing, 400715, PR China
[d] Sorbonne Université, Centre National de la Recherche Scientifique CNRS, Physico-chimie des Electrolytes et Nanosystèmes InterfaciauX, PHENIX, F-75005, Paris, France

HIGHLIGHTS

- PECVD is a promising technology for depositing APTES.
- A high amine proportion can be obtained by adjusting plasma parameters.
- As-deposited APTES film is in favor of assembling particles at near-nano size.

ARTICLE INFO

ABSTRACT

Although solid particles assembling on substrate surface is one of the key points for developing membrane reactors, the technology of organizing nano/near nanometer building blocks into complex structures is still a challenge to scientists in years. In this work, amine functional groups were deposited on the surface of different substrates *via* plasma enhanced chemical vapor deposition (PECVD) technology and (3-aminopropyl)triethoxysilane monomers were used as precursors. The influence of active gas, substrates, as well as deposition time on the physico-chemical features of as-deposited film were investigated, respectively. The highest density of amine of 5.5% on surface was obtained when Ar was utilized as active gas and deposition time was 40 s. Furthermore, Y type zeolite particles at near-nano size were synthesized and subsequently used as a model material for testing the immobilizing ability of plasma treated surface. The results clearly confirmed that a dense mono or multi-layer of closely packed zeolite particles could be formed on the APTES as-deposited surface after 24 h' immersion and the surface area of substrate could be improved by the deposition of zeolite.

1. Introduction

The key point for fabricating catalytic membrane reactors is to functionalize its surface to immobilize packed solid catalyst particles [1–3]. Although the technology of organizing molecules building blocks into complex structures has become common for scientists in recent years. The ability of well-controlling building blocks in bigger size has not yet been acquired. Especially, the catalytic particles with a usual size >100 nm is facing many obstacles for their further application. On one hand, it is difficult to find a suitable functional group with high attaching ability and good stability; on the other hand, there is still much left for improving the technologies of functionalization. Concerning the variation of raw materials for the fabrication of reactor substrates [4–6], functionalization using organosilane with –NH2, –SH, –COOH … are taken into account [7–12]. Especially, (3-aminopropyl)triethoxysilane (APTES) that provides a terminal amine functional group in each molecule was widely used in this decades [11,13–15]. However, the functionalization with APTES is often carried out in a conventional way, which is assistant with a wet-chemistry treatment of surface hydroxylation and ethoxy hydrolysis [16,17], showing many disadvantages: 1)
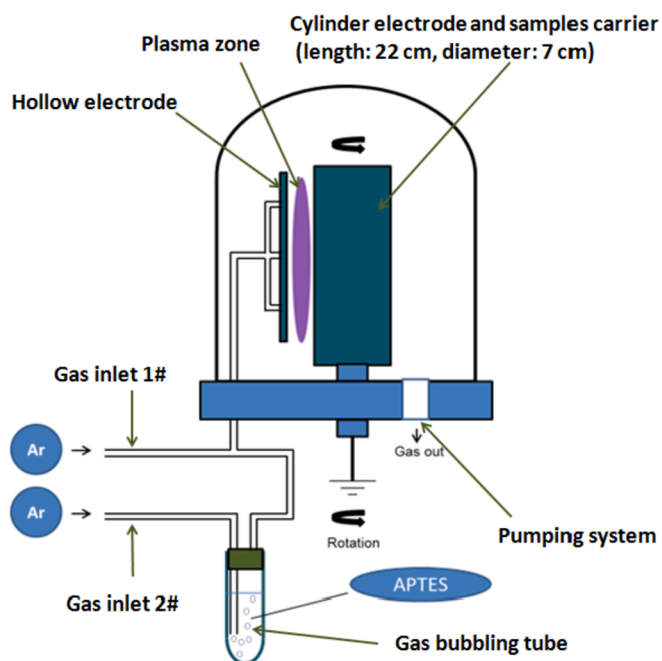

Fig. 1. The setup of plasma device used in this work.

the treatment method varies from an experimenter to another one, which results in the reduction of the reproducibility; 2) the protocol of treatment usually includes several steps, which means it is time consuming and low efficient; 3) the pretreatment with acids is necessary for activating surface, which would limit the scope of substrate materials; 4) the final surface state of the modified substrate is sensitive and may vary with experimental conditions, *e.g.* temperature, presence of water, concentration of APTES [18–20].

Alternatively, plasma enhanced chemical vapor deposition method, which is also called PECVD method, is showing promising potential due to its advantages of high reproducibility, high efficency and low-cost [21,22]. Especially, the plasma deposition process is always compaied with polymerizaiton [23–25], implying an additional improvement of stability and adhesion strength of organosilane films. In spite that a few papers concerning the functionalization of surface using PECVD method with APTES have been relased in recent years [26–32], the characteristics of as-deposited film *e.g.* the chemical structure, the amine density, *etc.* corresponding to the plasma parameters like gas selection, deposition time, substrate materials, as well as the ability of APTES layers for anchoring nano/near-nano particles have not been systemically investigated until today.

Zeolite is considered as a specific catalyst of high sharp selectivity in some reactions due to its three-dimensional framework forming channels and/or cages with molecular dimension [33–36]. Besides, its large external surface area provides many reaction sites for heterogeneous catalytic reactions taking place. In other words, zeolite could also be used as a support material that could atomically disperse the other nano catalysts with a high degree of uniformity [37,38]. The utilization of assembled zeolites and/or nano catalysts immobilized zeolites in microfluidic system consisted with the advantages of membrane and microreactor has expanded the applications in heterogeneous catalysis in this decade [39–45]. Recently, zeolite was reported to be used in the investigation of organizing nano to micrometer-sized building blocks on surface [46,47], showing that it could be a model material to test the immobilizing ability of as-functionalized substrates.

In this work, a thin film containing amine groups was deposited by PECVD method with precussor of APTES monomers. In order to maintain amines with high density, the characteristics of as-deposited films were varied by using different gas, substrate and deposition time.

Thereafter, water contact angle meter (WCA), X-ray photoelectron spectroscopy (XPS), Fourier transform infrared (FTIR) spectroscopy and ellipsometry measurements were used for characterizing the surface energy, chemical structure and thickness of as-deposited films. For confirming the immobilizing ability of PECVD treated surfaces, typical catalytic particles (zeolite) at near-nano size were immobilized on the topmost of the substrate surface with as-deposited APTES film.

2. Experimental

2.1. Materials and chemicals

Glass, Cyclic Olefin Copolymer (COC) and silicon were used as substrates with a dimesion of 8 mm × 8 mm × 1 mm (3-aminopropyl)triethoxysilane (APTES), carboxyethylsilanetriol sodium (CES) and toluene were purchased from VWR.Co; ethanol and acetone were purchased from Sigma-Aldrich. Ar, O_2 and N_2 gas with a purity of 99.99% were used as active gas for PECVD process.

2.2. Deposition of APTES by PECVD method

A bell type homemade plasma device was used for APTES depostion. The setup of this device was depicted in Fig. 1 and the details was introduced in our previous work [48]. The samples were fixed on the center of a rotating cylinder for deposition. 10 sccm of Ar was initially introduced into the chamber for pretreatment, the samples were activated using a voltage of 20 W under the gas pressure of 0.7 bar for 5 s. Thereafter, the as-activated samples were deposited with APTES for maintaining amine groups. A gaseous mixture consisted with of 20 sccm of active gas (Ar, O_2 or N_2) and 10 sccm of vector gas (Ar) carrying APTES was injected into the reaction chamber. During deposition, the pressure in chamber was fixed at 0.5 mbar and the power was 25 W, the APTES was heated at 80 °C in a gas bubbling tube, the reaction time was varied from 5 s to 80 s.

2.3. Assembling catalytic particles on APTES as-deposited surface

Y type zeolite was used as a model material for the test of immobilizing ability of APTES as-deposited surfaces. The zeolite with a diameter of about 100–150 nm was synthesized according to the method reported by Creaser et al. [49]. Subsequently, 100 mg of as-synthesized Y type zeolite powders and 200 μL of carboxyethylsilanetriol sodium (CES) were magnetically stirred with 30 mL of toluene at 120 °C for 4 h. The as-reacted zeolite powders were repeatedly washed by centrifuge to clean up unreacted CES, and then were dried at 100 °C. Meanwhile, APTES was deposited on COC surface that was deposited with APTES using PECVD. Thereafter, 50 mg of as-dried zeolite powers were magnetically mixed with 20 mL of Millipore water in a beaker, the plasma treated COC were then fixed at the bottom of beaker for 2 min, 10 min, 1.5 h, 3 h, 6 h, 12 h, 24 h and 48 h. During the immersion, the pH value of mixture was adjusted to 8.4. The zeolite deposited COC substrates were then dried at 80 °C.

2.4. Characterizations

A GBX-3S processing system (GBX, France) was used for capturing static water contact angle (WCA) of as-deposited surfaces. In order to test the stability of the APTES films, each sample was rinsed for 30 s by deionized water, dried by compressed air flow and evaluated afterwards. A Tensor 27 spectrometer (Bruker, UK) equipped with a deuterated triglycine sulphate (DTGS) was employed for collecting the Fourier transform infrared (FTIR) spectra, the recording range was from 4000 to 600 cm^{-1}. A PHI 5600-ci XPS spectrometer (Physical Electronics, USA) was used for collecting XPS spectra. For survey spectra, the anode used was a monochromatic Al Kα (1486.6 eV) X-ray sources at 200 W. For high resolution spectra, the anode used was a monochromatic Mg Kα
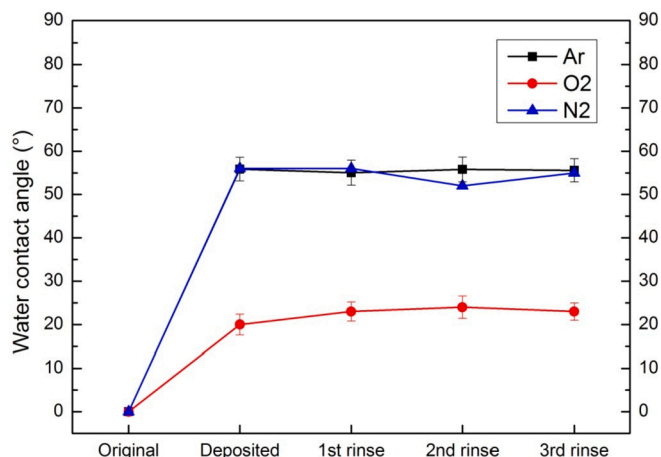
Fig. 2. WCA results of glass surface deposited with APTES using different active gas.

(1253.6 eV) X-ray sources at 200 W. Analysis were performed with a 45° angle from the surface. The analyzed surface area was 0.005 cm^2. Curve fitting for the high resolution C_{1s} core level peaks was done by using the XPS PEAK software (version 4.1) by means of a least square peak fitting procedure using a Gaussian-Lorentzian function (30% Lorentzian) and a Shirley baseline fitting. The quality of the peak syntheses was evaluated by the maximal residual standard deviation (residual STD) method. An analysis was considered significant if the residue was close to unity. On

each sample, three different spots were analyzed. Finally, the binding energy scale was corrected for the neutralizer shift by using the C_{1s} signal from saturated hydrocarbon at 285.0 eV as an internal standard. Depending on the carbon bond and its more or less electron negative partner, the carbon groups were assigned to the corresponding positions. Consequently, the FWHM with consistent value and position constraints were forced for fitting. A UVISEL spectroscopic ellipsometer (Horiba, Japan) was used for the measurement of film thickness from the range of 250–830 nm at an incident angle of 75°.

3. Results and discussion

3.1. Influence of active gas

As the most frequently utilized active gases for plasma deposition [28,29], Ar, O_2 and N_2 were respectively introduced into the chamber when APTES was deposited on glass for 5 s. The WCAs of APTES deposited surface using different active gas are presented in Fig. 2. A significant increase of WCAs was observed after APTES deposition, indicating the chemical structure changes on the topmost of glass substrate. Concerning alkane groups with high hydrophobicity existing in APTES molecule, the increase of WCA could correspond to the successful deposition of films with APTES [50]. Moreover, different active gas showed variation as $WCA_{Ar} = 55.9° \pm 0.7$, $WCA_{N2} = 56.0° \pm 1.2$ while $WCA_{O2} = 20° \pm 2.4$. The lower hydrophobic surface is probaly due to the oxidation of more alkane groups in O_2 plasma. Furthermore, the stability of as-deposited films were investigated. A tiny change of WCA ($<5°$) was seen even after 3 times of rinses on each film, confirming a good stability
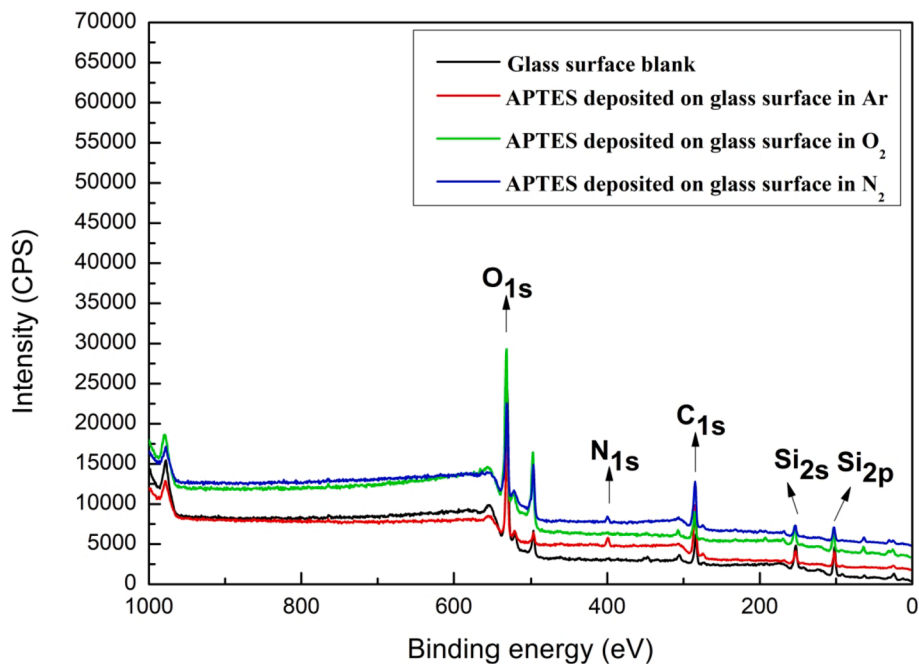

Fig. 3. XPS survey spectra of glass surface deposited with APTES using different active gas.

Table 1
XPS measurements of glass surface deposited with APTES using different active gas.

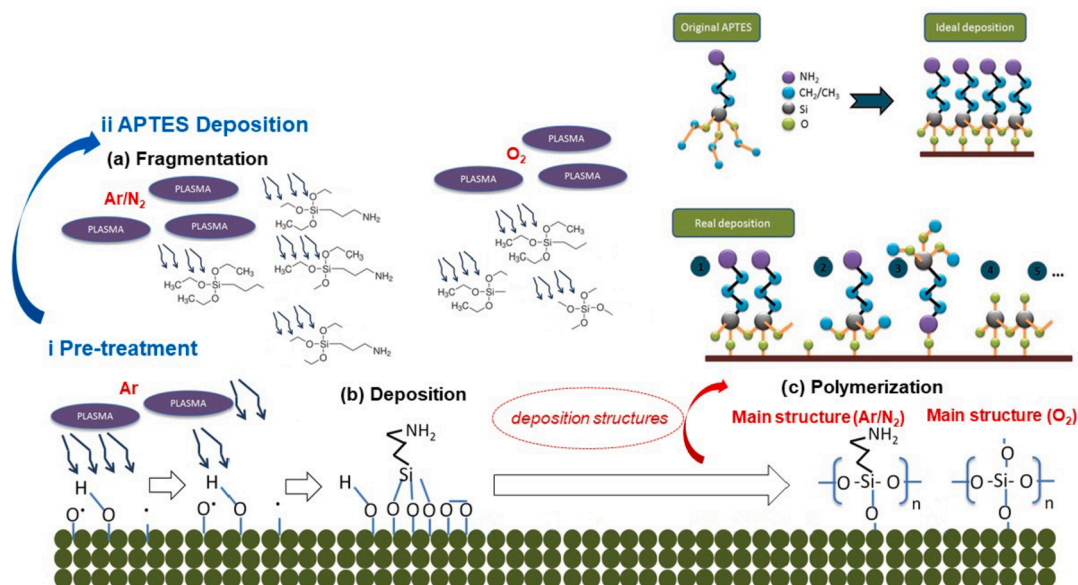| Sample type	O (at. %)	C (at. %)	Si (at. %)	N (at. %)	Na (at. %)	O/Si	C/Si	N/Si
Original glass	52.3 ± 0.2	23.8 ± 0.3	19.5 ± 0.4	0.7 ± 0.3	3.8 ± 0.2	2.7	1.2	0.04
Theoretical APTES	–	–	–	–	–	3	9	1
Tripod structure APTES	–	–	–	–	–	3	3	1
APTES in Ar	34.5 ± 0.3	48.4 ± 0.4	10.2 ± 0.2	5 ± 0.3	1.9 ± 0.1	3.4	4.7	0.49
APTES in O_2	51.4 ± 0.1	22.3 ± 0.3	14.3 ± 0.2	0.4 ± 0.1	11.6 ± 0.4	3.6	1.6	0.03
APTES in N_2	36.2 ± 0.4	42.3 ± 0.4	8.9 ± 0.2	3.9 ± 0.2	8.7 ± 0.4	4.1	4.8	0.44

Fig. 4. Mechanism of plasma depositing APTES molecules on surface using different active gas.

resisting water has been achieved during plasma deposition.

The survey scans of APTES deposited surface using different active gas are shown in Fig. 3 and Table 1. The XPS results indicated the changes of chemical composition of films when different active gas was used. The higher contents of nigtrogen and carbon, as well as the lower content of oxygen and silicon, were detected from the films deposited in Ar and N_2, respectively, evidencing a successful deposition of APTES on glass surface. In contrast, the high contents of oxygen and silicon, as well as the lower content of nigtrogen and carbon were observed from the film deposited in O_2. The surface compositions (see Table 1) between original glass and O_2 plasma treated one were quite similar. As the glass is mainly consisted with SiO_2, it could be related to the formation of SiO_2-like structures in O_2 plasma as a result of oxidizing $-CH_2CH_2CH_2-NH_2$ and/or $-CH_2CH_3$ by oxygen radicals [29]. The results were also in accordance with previous WCA measurements, as a lower hydrophobic surface could be achieved due to the formation of more hydrophilic SiO_2-like structures by using O_2.

Interestingly, the films deposited in Ar and N_2 also exihibited higher content of oxygen than that of unreacted APTES (at.%O_{Ar} = 34.5, at.% O_{N2} = 36.2 vs at.%O_{report} = 21.72 [16]), implying APTES molecules are partially oxidized in Ar or N_2 plasma. Accordingly, the higher O/Si ratios calculated from the films deposited in Ar and N_2 (O/Si$_{Ar}$ = 3.4, O/Si$_{N2}$ = 4.1 vs O/Si$_{unreacted\ APTES}$ = 3) were obtained. The oxidation could be attributed to the excitation of residual O_2 by Ar or N_2 plasma. The O/Si ratio of film deposited in O_2 was seen lower than that deposited in N_2 (O/Si$_{O2}$ = 3.6 vs O/Si$_{N2}$ = 4.1). However, it is noticed that on one hand the high O/Si ratio corresponds to a higher O content exists in as-deposited film, on the other hand it could also be contributed to a lower Si content. In Table 1, the content of O in the film deposited using O_2 plasma was much higher than that of using N_2 plasma (at.% O_{O2} = 51.4 vs at.%O_{N2} = 36.2), while the content of Si in the film deposited using N_2 plasma was much lower than that using O_2 plasma (at.%Si_{N2} = 8.9 vs at.%Si_{O2} = 14.3), leading to a lower O/Si ratio of film deposited in O_2. However, higher O and Si contents exist in the film could correspond to the formation of more SiO_2-like structures, in accordance with our speculation. Furthermore, the C/Si and N/Si ratios of films deposited in Ar and N_2 were significantly lower than that of unreacted APTES (C/Si$_{Ar}$ = 4.7 and N/Si$_{Ar}$ = 0.49, C/Si$_{N2}$ = 4.8 and N/Si$_{N2}$ = 0.44 vs C/Si$_{unreacted\ APTES}$ = 9 and N/Si$_{unreacted\ APTES}$ = 1), indicating a high crosslinking after deposition. It is notice that if a "tripod structure" of APTES, which forms three O–Si–O bonds by losing all the ethoxy groups in moleculer, are achieved during deposition, the C/Si

ratio should be 3. The higher C/Si ratio is observed, the more ethoxy groups exist in the film. Thus, the high C/Si ratios indicated that not all the APTES molecules have perfectly bonded to surface through three siloxane bonds in Ar or N_2 plasma. The APTES molecule could lose only one or two ethoxy groups from the three tails; alternatively, it could also keep three ethoxy groups and attach to the surface through the interaction between amine and hydroxyl groups [18]. According to literature [51–54], the organosilanes, as used herein for surface functionalization, are able to polymerize, especially in the presence of plasma, forming a number of possible 2D and 3D surface structures. Thus, APTES molecules deposited on the surface could enable the appearance of various surface structures. It means the APTES film deposited on surface could mainly bind with Si to the substrate and also partially bind with N to the substrate.

The surfaces of substrates are initially pre-treated with Ar plasma. Since the oxygen presents as trace in the reactor is excited by plasma in pre-treatment, the surface is activated with oxygen radicals and hydroxyl radicals. Then APTES monomers are introduced in the chamber and fragmented by plasma. As plasma power is employed, the electric field between electrodes begins to generate free electrons and ions, that are subsequently accelerated leading to collisions with APTES monomer molecules. The monomer molecules are excited to higher energy states, primarily by inelastic collisions with the energetic electrons, and decomposed into fragments (i.e. radicals, ions, atoms and more electrons). Thereafter, the fragments of APTES molecules move to the substrate and subsequently bind to the substrate surface through the interaction between ethoxyl group and oxygen/hydroxyl radicals, as shown in Fig. 4. When deposition is processed, APTES fragments continuously bind to each others and form an amorphous polymerized film [21,28]. However different active gas could lead to the formation of different layers: deposition in Ar or N_2 plasma forms a layer with the similar chemical structure that corresponds to the feature of APTES, which could be contributed to that argon and nitrogen radicals are not reactive species for organosilanes. As the binding energy of chemical chains of APTES molecule varies [55], APTES monomers are fragmented into various forms. Thus, the as-deposited layer should be consisted with different APTES structures [56,57]. When Ar or N_2 is used, the as-deposited film is consisted with major APTES-like structures (Fig. 4 ①②③) and minor SiO_2-like structure (Fig. 4 ④). When O_2 is used, the as the as-deposited film is consisted with major SiO_2-like structure (Fig. 4 ⑤) and minor APTES-like structures (Fig. 4 ①②③).

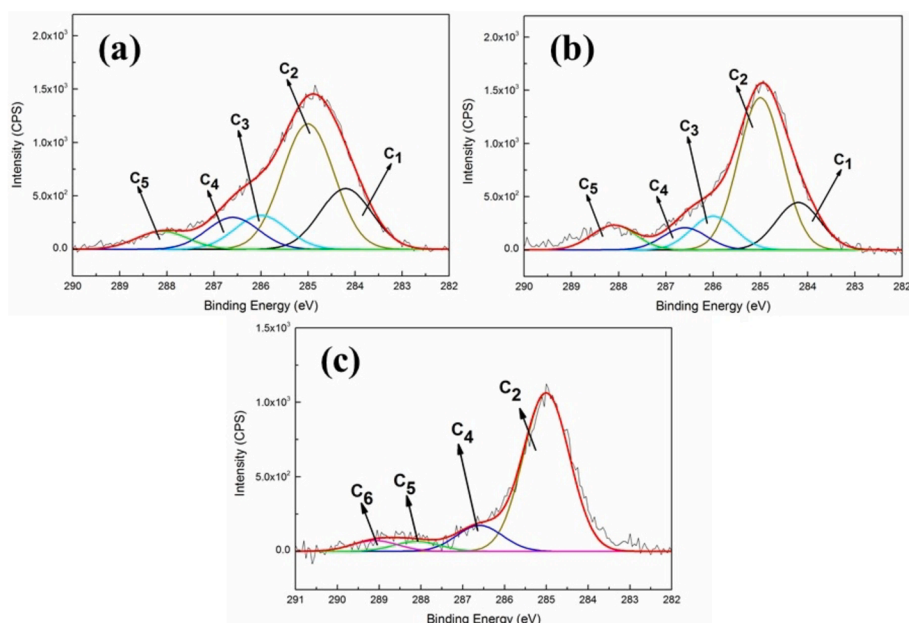The high resolution C_{1s} spectra of APTES deposited surface using

Fig. 5. High-resolution XPS spectra of glass surface deposited with APTES using different active gas: (a) Ar, (b) N$_2$, (c) O$_2$.

Table 2
Relative contribution of the deconvoluted components of the C$_{1s}$ peaks.

Active gas	C$_{1s}$						Amine (Relative to total composition, %)
	C$_1$ (%)	C$_2$ (%)	C$_3$ (%)	C$_4$ (%)	C$_5$ (%)	C$_6$ (%)	
Ar	20.1	53.0	10.4	11.5	5.0	–	5.0
N$_2$	13.3	63.7	9.3	7	6.7	–	3.9
O$_2$	–	82.8	–	7.8	2.6	6.8	–

different active gas are shown in Fig. 5. As seen in Fig. 5(a) and (b), C$_{1s}$ spectra obtained from the films deposited in Ar and N$_2$ could be deconvoluted into five peaks: a peak centered at 285.0 eV (C$_2$) corresponding to C–C, C=C and C–H groups; a lower binding energy (BE) peak centered at 284.2 eV (C$_1$) corresponding to C–Si; three higher BE peaks centered at 286 eV (C$_3$) 286.6 eV (C$_4$) and 288.1 eV (C$_5$), corresponding to C–N, C–O/C=N and N–C=O/C=O groups, respectively. The results are in accordance with that of as-reported APTES films [27]. Differently, the sample that aquired in O$_2$ plasma shows only C$_2$, C$_4$ and C$_5$ components with an absence of C$_1$ peak relating to C–Si groups and C$_3$ peak relating to C–N groups, indicating the oxidation of –CH$_2$CH$_2$CH$_2$NH$_2$ and –CH$_2$CH$_3$ when O$_2$ is used. Conerning there's still high content of silicon existing in the film, it could be resonably speculated that Si–CH$_2$CH$_2$CH$_2$NH$_2$ and Si–CH$_2$CH$_3$ have been oxidized and transfromed into SiO$_2$-like structure in O$_2$ plasma [29]. A new peak centered at 289.2 eV corresponding to O–C=O groups (C$_6$) was observed in this spectrum. It could also be attributed to the strong oxidation in O$_2$ plasma. Based on the components proportion in C$_{1s}$ (Table 2), the real proportion of C–N bond (C$_3$) in the film can be calculated using Equation (1):

$$\%_{C-N\ in\ coating} = C_{1s} \times \%C_3 \tag{1}$$

where C_{1s} is the content of carbon in film, $\%C_3$ is the proportion of C$_3$ bond in C$_{1s}$. Thus, the results indicated that Ar is the better active gas for obtaining amine groups (C-N$_{Ar}$ = 5.0% vs C-N$_{N2}$ = 3.9%.).

3.2. Influence of substrate

Three typical raw materials (glass, COC and Si) for fabricating membrane reactor were investigated, Ar was used as active gas and the
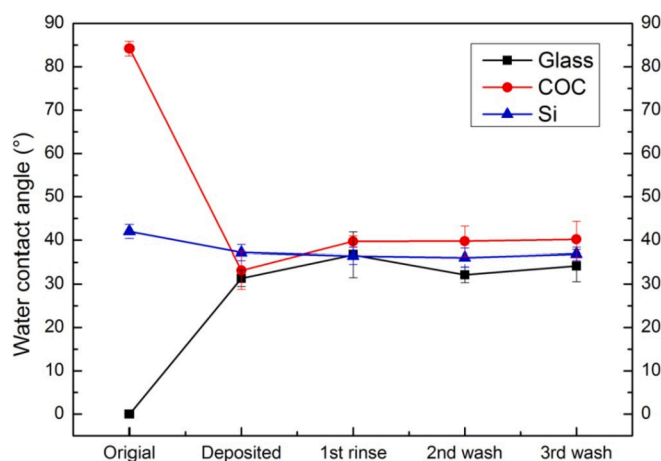

Fig. 6. WCA measurements of APTES film deposited on glass, COC and silicon.

deposition time was fixed at 40 s. WCA results presented in Fig. 6 indicated the similar hydrophility was achieved on different substrates. Furthermore, the similar stability resisting water of all the samples implied that the nature of substrates is not a key factor to affect the films's chemical properties.

FTIR spectra of APTES film deposited on different substrates showed the similar feature (Fig. 7). A strong absorption band at about 1050 cm^{-1}, corresponding to Si–O–C and Si–O–Si, could contribute to polymerized or physisorbed APTES molecules. Another band at the shoulder of 1150 cm^{-1} was probably due to short chain Si–O–Si as a result of cross-linking [58], while the band around 1050 cm^{-1} was assigned to the long chain Si–O–Si [29,30,48]. The bands corresponding to primary amine appeared in the range of 1400–1700 cm^{-1}: two vibrational modes at 1620 cm^{-1} and 1400 cm^{-1} were due to NH$_2$ group from APTES [21,23] and C–N bonds from amines or amides [29], respectively. The absorption band at 1750 cm^{-1} relating to C=O groups was also an evidence of amides. Thus, it indicated the oxidation of the amines to amide by residual oxygen radical during deposition. The asymmetric and symmetric deformation modes corresponding to CH$_2$ and CH$_3$ groups of ethoxy were seen around 2950 and 2870 cm^{-1},
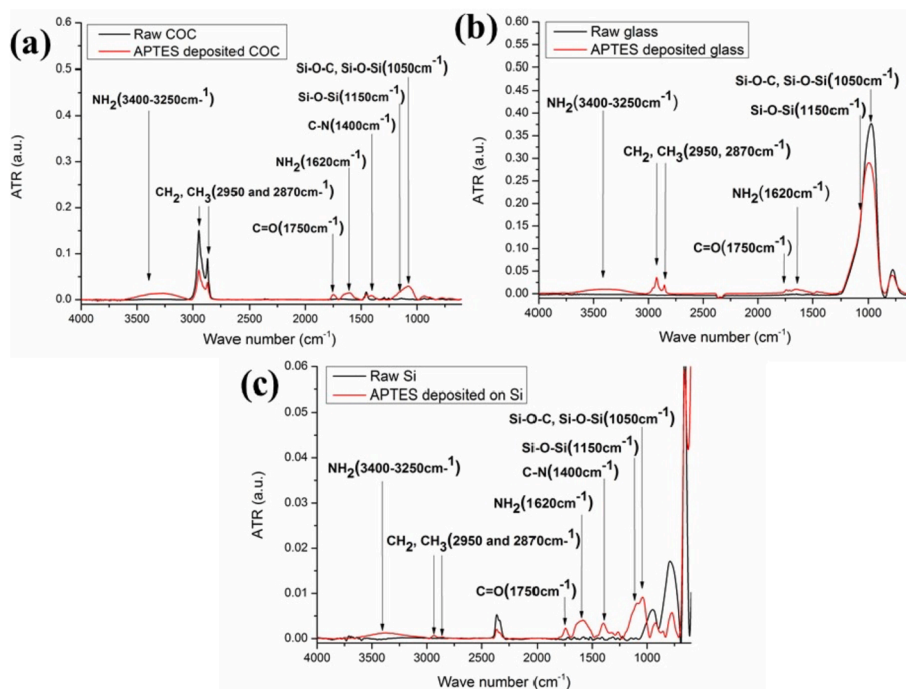
Fig. 7. FTIR spectra of APTES films deposited on various substrates: (a) Glass; (b) COC; (c) Si.

Table 3
XPS measurements of the chemical composition of APTES films deposited on glass, COC and silicon.

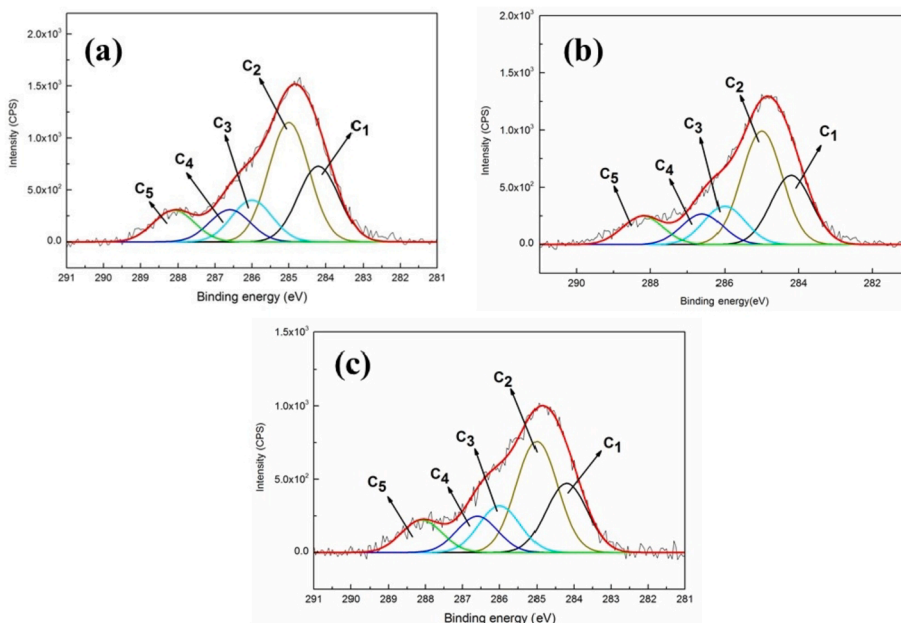| Substrate	O (at. %)	C (at. %)	Si (at. %)	N (at. %)	Na (at. %)	O/Si	C/Si	N/Si
Glass	36.6 ± 0.7	43.5 ± 0.3	11.2 ± 0.2	5.8 ± 0.3	2.9 ± 0.2	3.3	3.9	0.52
COC	34.3 ± 0.4	45.9 ± 0.2	12.9 ± 0.3	6.9 ± 0.3	–	2.7	3.6	0.53
Si	35.2 ± 0.1	40.2 ± 0.3	19.2 ± 0.1	5.5 ± 0.3	–	2.1	1.8	0.28

Fig. 8. High-resolution C_{1s} XPS spectra of APTES films deposited on various substrates: (a) Glass; (b) COC; (c) Si.

showing the existence of unhydrolyzed APTES. Moreover, the broad absorption band in the range of 3400–3250 cm^{-1} could also be assigned to the OH stretching of H_2O or symmetric/asymmetric NH stretching modes of APTES.

Furthermore, the elemental compositions of flims deposited on various substrates determined by XPS are shown in Table 3. The APTES films deposited on glass and COC presented similar O/Si, C/Si and N/Si ratio, indicating the same chemical structure are formed on both

Table 4
Relative contribution of the deconvoluted components of the C_{1s} peaks.

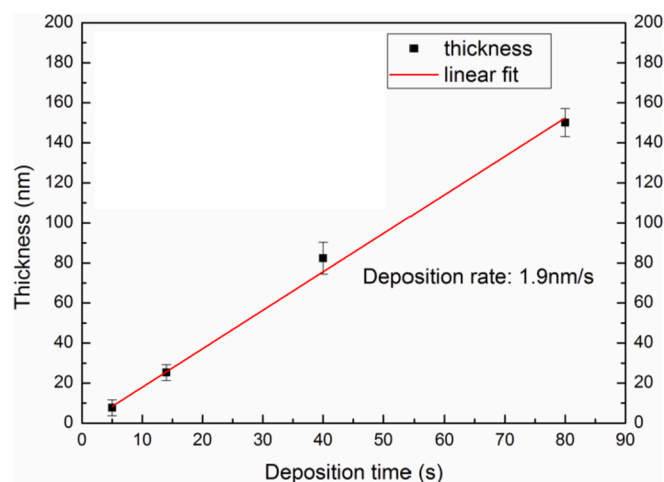| Substrate	C_{1s}					Amine (Relative to total composition, %)
	C_1 (%)	C_2 (%)	C_3 (%)	C_4 (%)	C_5 (%)	
Glass	23.2	44.8	12.7	8.7	10.5	5.5
COC	23.2	46.7	12.5	9.2	8.4	5.7
Si	22.5	40.8	13.8	12.9	10	5.5

Fig. 9. Analysis of the film thickness as a function of deposition time.

Table 5
Water contact angle and ellipsometry analysis of APTES film deposited for different time.

Deposition time (s)	Thickness (nm)	Water contact angle on different substrates (°)		
		Glass	COC	Si
5	7.7 ± 4	55.9 ± 0.7	50.9 ± 1.0	54.3 ± 0.6
14	25.3 ± 4	37.7 ± 1.7	39.9 ± 0.8	39.4 ± 0.5
40	82.4 ± 8	31.3 ± 1.9	33.2 ± 0.7	37.2 ± 1.0
80	150.1 ± 7	40.6 ± 0.5	49.3 ± 0.7	43.8 ± 1.0

substrates. The different ratios of O/Si, C/Si and N/Si acquired from Si surface are probably due to the contamination of the gas phase by etched silicon atoms from substrate. The further high resolution C_{1s} spectra confirmed the speculation as the same deconvoluted components with similar proportion are mantained from the three substrate surfaces. (*cf.* Fig. 8 and Table 4). All the results clearly indicated that plasma

polymerization leads to an efficient APTES deposition on all the substrates that are potential materials for reactor fabrication. Furthermore, similar amine contributions were obtained from the film on different substrates ($\%Amine_{glass} = 5.5$, $\%Amine_{COC} = 5.7$, $\%Amine_{Si} = 5.5$). If we consider the chemical structure of APTES, the hydrophilicity is mainly controlled by the amine group and the density of amine on the surface determines the WCA on surface. Thus, no obvious change of hydrophilicty could be detected on various substrates in Fig. 6, in accordance with XPS results.

3.3. Influence of deposition time

As shown in Fig. 9 and Table 5, the film thickness changed as the deposition time varied during 5–80 s and the average growth rate was about 1.9 nm/s. The WCAs on three different substrates showed the similar trend of change: WCAs decreased during 5–40 s and then followed by a slight increase. It is known to all, the number of active species gerated from precursor molecules increases with a raise of deposition time. Thus, the more amine groups are obtained with an increase of time. However, the longer time also increases the risk that as-deposited film exposes to plasma, which subsequently leads to bombardment of the reactive polar groups. Finally, the over-treatment of film changes the polarity of molecules and casues the increase of WCAs on surface.

The FTIR spectra of APTES flims deposited on COC using different time presented in Fig. 10 highlighted the changes of chemical bonds. As a result of improving film thickness, the peak in the range of $3400–3250\ cm^{-1}$ corresponding to the symmetrical/asymmetrical NH stretch modes increased with a raise of deposition time (Fig. 10(a)). However, the intensity of peak at $1750\ cm^{-1}$ relating to carboxylate functions showed different trend (Fig. 10(b)):

$$I(C=O)_{5s} < I(C=O)_{80s} < I(C=O)_{14s} < I(C=O)_{40s}$$

Besides, the peaks in the range of $1650–1590\ cm^{-1}$ were attributed to N–H bending (scissoring) vibration of primary amines [59]. Interestingly, an increase of peak intensity as well as peak center shifting to higher frequency with a raise of deposition time was observed, indicating the increase of the free amine transformed from H-bonded amine [21,60]. When the deposition time was extended to 80s, the peak center shifted to $1660\ cm^{-1}$. The band could be assigned to the vibrational mode of amide/imine/oxime, which is probably due to the intensive oxidation induced by long time exposure to plasma [29,58].

Furthermore, the XPS analyses were performed and the results are shown in Table 6. The content of carbon decreased with an increase of nitrogen, indicating the formation of a more inorganic film by increasing deposition time. The highest C/Si ratio and the lowest N/Si ratio were obtained when the deposition time was 5 s, indicating an insufficient polymerization. The results suggested the deposition time for APTES in our system should be longer than 5 s.
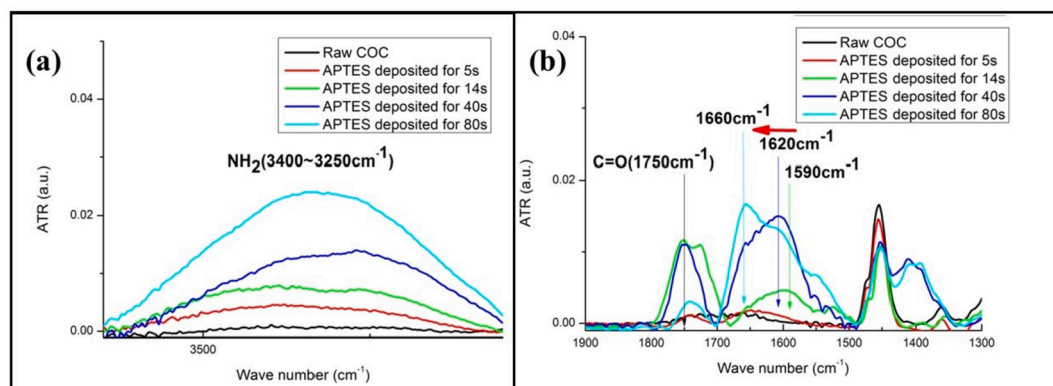

Fig. 10. FTIR spectra of APTES films deposited on COC using different time: (a) high wavenumber scanning region; (b) low wavenumber scanning region.

Table 6

XPS data of APTES films deposited on glass using different times.

Deposition time (s)	O (at. %)	C (at. %)	Si (at. %)	N (at. %)	Na (at. %)	O/Si	C/Si	N/Si
5	34.5 ± 0.3	48.4 ± 0.4	10.2 ± 0.2	5 ± 0.3	1.9 ± 0.1	3.4	4.7	0.49
14	33.9 ± 0.3	43.1 ± 0.3	11.5 ± 0.3	5.6 ± 0.3	5.6 ± 0.4	3.0	3.7	0.49
40	36.6 ± 0.1	43.5 ± 0.3	11.2 ± 0.3	5.8 ± 0.1	2.9 ± 0.0	3.3	3.9	0.52
80	33.2 ± 0.8	42.6 ± 0.3	11.3 ± 0.4	5.9 ± 0.2	7.1 ± 0.1	2.9	3.8	0.52

Table 7

Relative contribution of the deconvoluted components of the C_{1s} peaks.

Deposition time (s)	C_{1s}					Amine (Relative to total composition, %)
	C_1 (%)	C_2 (%)	C_3 (%)	C_4 (%)	C_5 (%)	
5	20.1	53.0	10.4	11.5	5.0	5.0
14	21.9	49.1	12.4	7.9	8.7	5.3
40	23.2	44.8	12.7	8.7	10.5	5.5
80	23.4	47.1	11.3	10.2	8.0	4.8

The proportions of each components contributed in C_{1s} spectrum as a function of deposition time are shown in Table 7. A sharp decrease of C–O/C=N content (C_4) was seen when deposition time was longer than 5 s. It could be contributed to Si–O–CH_2CH_3 of APTES forming siloxane bond, evidencing more crosslinking occurs after 5 s. Thereafter, C–O content increased with a raise of deposition time during 14–80 s, indicating an increase of imine or oxime. The C=O content (C_5) increased with a raise of deposition time. However, a strong decline was seen after 40 s. All the results were in accordance with the FITR spectra as shown in

Fig. 9(b). The highest C–N content (5.5%) in film was obtained when the deposition time was 40 s.

In order to confirm the high efficiency of using plasma method, the glass substrates were functionalized with APTES in a wet-chemistry way [61]. The results of survey scan, high-resolution spectrum and contribution of each component are shown in Fig. 11. Base on these results, the real proportion of C–N bond (C_3) in the film corresponding to amine density could be calculated. The amine density obtained by wet-chemical treatment was about 3.6%. Thus, the density of amine deposited using plasma was obviously higher than that of using wet-chemistry (%Amine$_{plasma}$ = 5.5 vs %Amine$_{wet-chemistry}$ = 3.6) in this work. Furthermore, a decrease of C–N content was seen as the deposition time was 80 s. The longer deposition time could rise the risk of exposing topmost of as-formed film to plasma, and subsequent leads to a functional change of film [58]. Thus, the deposition time is suggested to be in the range of 14–40s, in accordance of FTIR results.

3.4. Particles anchoring on APTES as-deposited surfaces

In order to estimate the potential of APTES deposited surface for
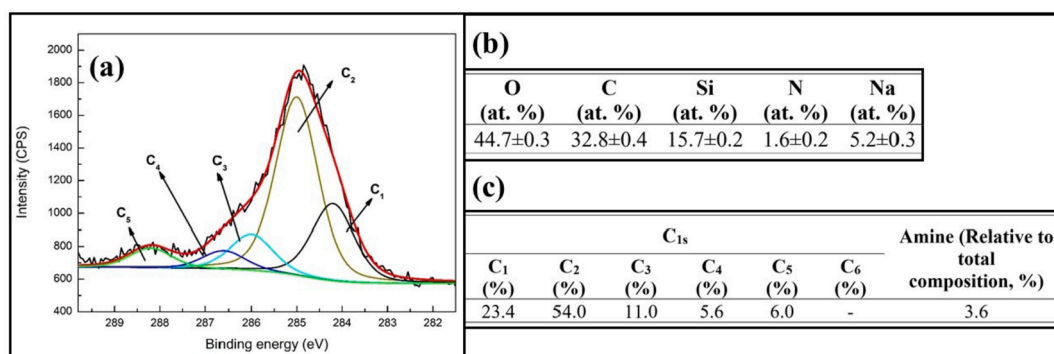

Fig. 11. (a) High-resolution C_{1s} XPS spectrum of glass surface deposited with APTES using wet-chemical treatment; (b) XPS measurements of glass surface deposited with APTES using wet-chemical treatment; (c) relative contribution of the deconvoluted components of the C_{1s} peaks.
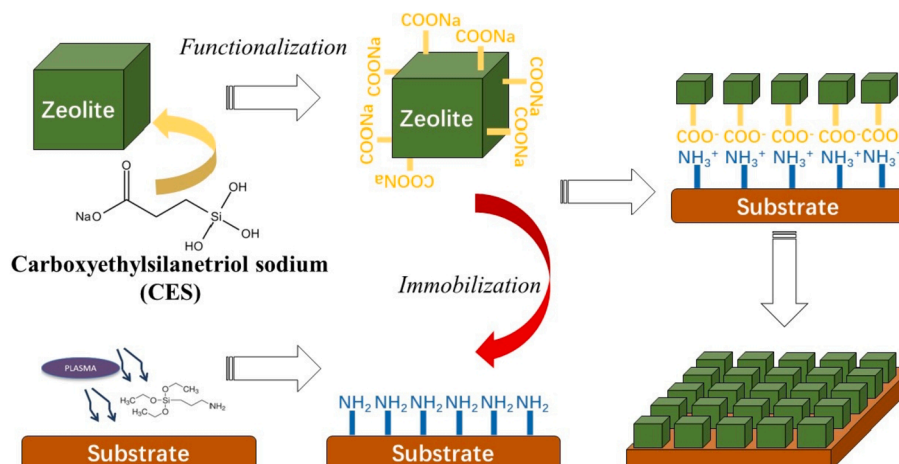

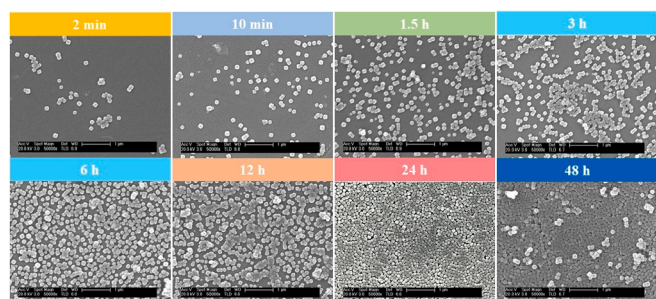**Fig. 12.** The process of immobilizing zeolite on APTES deposited surface.

Fig. 13. Morphology of COC surface immobilized with Y zeolite using different immersion duration.

making membrane reactors, Y type zeolites were used as a model material and were immobilized on the COC surface deposited with APTES (active gas: Ar, deposition time: 40 s). Carboxyethylsilanetriol sodium (CES) has been reported a promising linkage reagent as the uniform carboxylate group distributions on surface could endow high negative charges density at some pH value [62]. As presented in Fig. 12, zeolite particles were functionalized using CES in our work; meanwhile COC substrate was plasma polymerized with APTES for endowing amine groups on its surface. Based on the $pKa_{COOH} = 2.5$ and $pKa_{NH2} = 10.6$, massive $-COO^-$ and $-NH_3^+$ were respectively generated on the surface of zeolite and COC in a suspension of $pH = 8.4$. Thereafter, zeolite particles were immobilized on COC surface through the $-NH_3^+/-COO^-$ zwitterionic pairs [63].

As presented in Fig. 13, the degree of zeolite coverage varied from very scarce to very dense. In the early immersion period of 2–10 min, a few particles appeared on surface with very low coverage, indicating the seeding procedure occurs and the number of seeded zeolite particle raises with increasing time. As the immersion duration was extended to 1.5–3 h, the as-seeded zeolite particles tended to attach free zeolite particles in suspension, forming closely packed island-like precipitants. Meanwhile, as-deposited zeolites migrated and assembled on the surface, forming the same structure. Then the closely pack precipitants grew with an increase of immersion duration of 6–12 h. Finally, the surface was fully covered by a dense coating consisted with packed zeolite particles after 24 h's immersion. Furthermore, the longer immersion duration of 48 h showed little difference, suggesting 48 h's immersion is in favor of forming a multilayer, while 24 h's immersion is suitable for fabricating a monolayer.

FTIR spectra of zeolite immobilized surfaces treated using different immersion duration are shown in Fig. 14(a). A band corresponding to Si–O in SiO_4 tetrahedron was obtained from all the samples, indicating the existence of zeolites. XPS spectrum of Y zeolite immobilized surface immersed for 24 h is presented in Fig. 14(b). In comparison of APTES as-

deposited surface, characteristic peaks relating to Na_{1s}, Al_{2s} and Al_{2p}, as well as the increase of Si_{2s} and Si_{2p} peak intensity were seen, confirming the successful immobilization of zeolites, in agreement with FTIR results. Moreover, the variation of FTIR evidenced the increase of zeolite with a raise of immersion duration from 2 min to 48 h, as the improvement of Si–O band was observed. The higher intensity of Si–O peak obtained using 48 h's immersion, implied the increase of zeolite coating thickness due to the formation of multilayer.

A comparison experiment was carried out by immobilizing zeolite on the surfaces that were deposited with APTES and without APTES (immersion time: 48 h). The morphology of different surfaces are shown in Fig. 15. It was obviously seen that the feature of COC surface had been totally changed and the roughness of surface increased after immobilizing zeolite on APTES deposited surface, indicating an enhancement of surface area. The increase of surface area suggested that zeolite immoblized surface could be used for improving catalytic performance of membrane reactors or microreactors in dynamic solvents [1–3,13].

4. Conclusion

Thin polymerized films with high density of amine functional groups were deposited on surface using a PECVD method with APTES precussors. The films on various substrates showed similar chemical
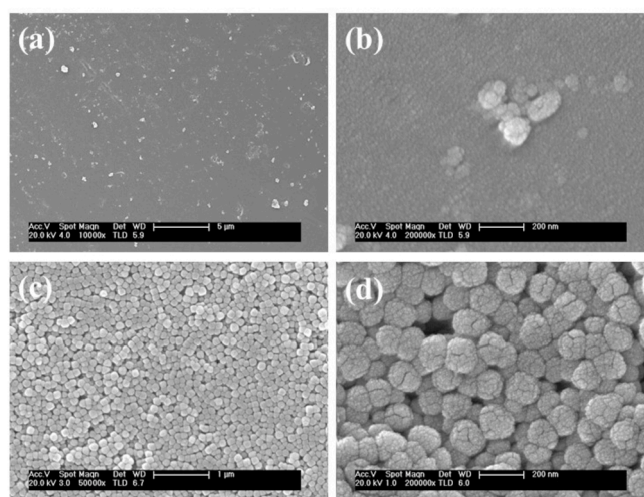

Fig. 15. Surface morphology of COC immobilized with zeolite (immersion time: 48 h): (a) COC without APTES, low magnification; (b) COC without APTES, high magnification; (c) COC with APTES, low magnification; (d) COC with APTES, high magnification.
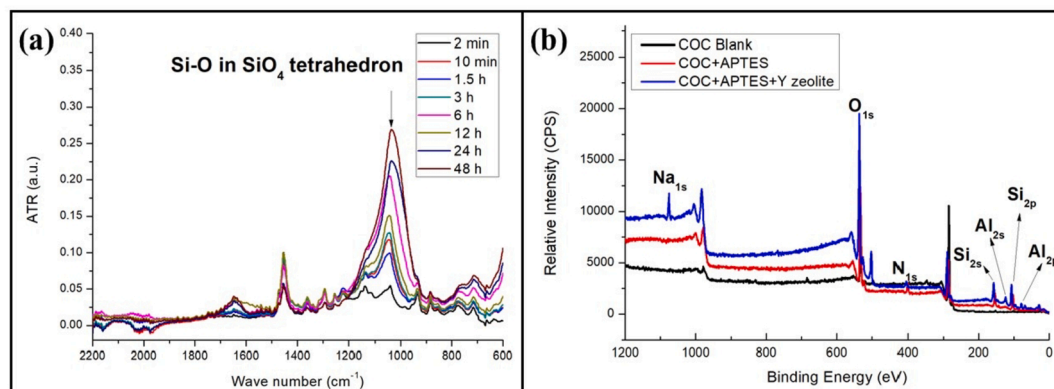

Fig. 14. (a) FTIR spectra of COC surface immobilized with Y zeolite using different immersion duration; (b) Survey XPS spectra of COC, APTES deposited COC and Y zeolite immobilized COC (24 h's immersion).

structure realted to APTES, evidencing that PECVD was a universal method for depositing APTES regardless of substrate nature. O_2 was confirmed a negative active gas for APTES plasma deposition, as massive SiO_2-like structures were generated by oxygen radicals. In comparison of N_2, amines deposited in Ar showed the higher density. Furthermore, The results showed the change of film characteristics with increasing deposition time. In order to avoid long exposure time to plasma, the deposition time should not be longer than 40 s. Under the conditions of $Q_{APTES} = 10$ sccm, $Q_{Ar} = 20$ sccm, $P = 25$ W, $p = 0.5$ mbar, $t = 40$ s, the maximum amine proportion of 5.5% was obtained in this work. Y type zeolite particles at near-nano size were then immobilized on the APTES deposited surface using different immersion duration (2 min-48 h), and the results proved plasma deposited amine was in favor of assembling near-nano particles, as a dense mono or multi-layer consisted with packed zeolites was detected after 24 h's immersion. The increase of surface area on APTES deposited COC substrate suggested that zeolite immoblized surface could be used for improving catalytic performance of membrane reactors or microreactors in the future.

Acknowledgements

References

[1] H. Yin, et al., Generation and extraction of hydrogen from low-temperature water-gas-shift reaction by a ZIF-8-based membrane reactor, Microporous Mesoporous Mater. 280 (2019) 347–356.

[2] Y. Zhang, et al., All-silica DD3R zeolite membrane with hydrophilic-functionalized surface for efficient and highly-stable pervaporation dehydration of acetic acid, J. Membr. Sci. 581 (2019) 236–242.

[3] A.D. Kiadehi, M. Taghizadeh, Fabrication, characterization, and application of palladium composite membrane on porous stainless steel substrate with NaY zeolite as an intermediate layer for hydrogen purification, Int. J. Hydrogen Energy 44 (5) (2019) 2889–2904.

[4] H. Li, et al., Highly efficient Suzuki cross-coupling reaction within an open channel plastic microreactor immobilized with palladium complexes, Microfluid. Nanofluidics 12 (6) (2012) 981–989.

[5] M.N. Tahir, et al., Continuous process for click reactions using glass micro-reactor functionalized with β-cyclodextrin, Tetrahedron Lett. 54 (25) (2013) 3268–3273.

[6] J. Ye, et al., Microcontact electrochemical etching technique for rapid fabrication of glass-based microfluidic chips, RSC Adv. 3 (19) (2013) 6960–6963.

[7] J. Huang, et al., 3-Aminopropyl-triethoxysilane functionalized graphene oxide: a highly efficient and recyclable catalyst for knoevenagel condensation, Catal. Lett. 145 (4) (2015) 1000–1007.

[8] M. Ben Haddada, et al., Optimizing the immobilization of gold nanoparticles on functionalized silicon surfaces: amine- vs thiol-terminated silane, Gold Bull. 46 (4) (2013) 335–341.

[9] E. Karaoglu, et al., Synthesis and characterization of catalytically activity Fe3o4–3-Aminopropyl-triethoxysilane/Pd nanocomposite, J. Inorg. Organomet. Polym. Mater. 23 (2) (2013) 409–417.

[10] K.N. Plunkett, et al., Light-regulated electrostatic interactions in colloidal suspensions, J. Am. Chem. Soc. 127 (42) (2005) 14574–14575.

[11] Z. Zhang, et al., A promising combo gene delivery system developed from (3-aminopropyl)triethoxysilane-modified iron oxide nanoparticles and cationic polymers, J. Nanoparticle Res. 15 (5) (2013) 1–11.

[12] F. Zhang, et al., Chemical vapor deposition of three aminosilanes on silicon dioxide: surface characterization, stability, effects of silane concentration, and cyanine dye adsorption, Langmuir 26 (18) (2010) 14648–14654.

[13] J. Ftouni, et al., Immobilization of gold nanoparticles on fused silica capillary surface for the development of catalytic microreactors, Chem. Eng. J. 227 (0) (2013) 103–110.

[14] B.-Z. Zhan, M.A. White, M. Lumsden, Bonding of organic amino, vinyl, and acryl groups to nanometer-sized NaX zeolite crystal surfaces, Langmuir 19 (10) (2003) 4205–4210.

[15] H. Li, et al., Aminosilane micropatterns on hydroxyl-terminated substrates: fabrication and applications, Langmuir 26 (8) (2010) 5603–5609.

[16] M. Qin, et al., Two methods for glass surface modification and their application in protein immobilization, Colloids Surfaces B Biointerfaces 60 (2) (2007) 243–249.

[17] J. Klug, et al., Chemical and electrochemical oxidation of silicon surfaces functionalized with APTES: the role of surface roughness in the AuNPs anchoring kinetics, J. Phys. Chem. C 117 (21) (2013) 11317–11327.

[18] R.G. Acres, et al., Molecular structure of 3-aminopropyltriethoxysilane layers formed on silanol-terminated silicon surfaces, J. Phys. Chem. C 116 (10) (2012) 6289–6297.

[19] Y. Mo, M. Zhu, M. Bai, Preparation and nano/microtribological properties of perfluorododecanoic acid (PFDA)–3-aminopropyltriethoxysilane (APS) self-assembled dual-layer film deposited on silicon, Colloid. Surf. Physicochem. Eng. Asp. 322 (1–3) (2008) 170–176.

[20] F. Zhang, M.P. Srinivasan, Self-assembled molecular films of aminosilanes and their immobilization capacities, Langmuir 20 (6) (2004) 2309–2314.

[21] C. Volcke, et al., Reactive amine surfaces for biosensor applications, prepared by plasma-enhanced chemical vapour modification of polyolefin materials, Biosens. Bioelectron. 25 (8) (2010) 1875–1880.

[22] Suhr, H., Applications and trends of nonequilibrium plasma chemistry with organic and organometallic compounds. Plasma Chem. Plasma Process.. 9(1): p. 7S-28S.

[23] I. Gancarz, et al., Plasma modified polymers as a support for enzyme immobilization II. Amines plasma, Eur. Polym. J. 39 (11) (2003) 2217–2224.

[24] J. Casimiro, et al., Introduction of primary amino groups on poly(ethylene terephthalate) surfaces by ammonia and a mix of nitrogen and hydrogen plasma, Plasma Chem. Plasma Process. 32 (2) (2011) 305–323.

[25] M. Asandulesa, et al., Chemical investigation on various aromatic compounds polymerization in low pressure helium plasma, Plasma Chem. Plasma Process. 34 (5) (2014) 1219–1232.

[26] F. Alba-Elías, et al., Tribological behavior of plasma-polymerized aminopropyltriethoxysilane films deposited on thermoplastic elastomers substrates, Thin Solid Films 540 (2013) 125–134.

[27] R.P. Gandhiraman, et al., High efficiency amine functionalization of cycloolefin polymer surfaces for biodiagnostics, J. Mater. Chem. 20 (20) (2010) 4116–4127.

[28] V. Gubala, et al., Functionalization of cycloolefin polymer surfaces by plasma-enhanced chemical vapour deposition: comprehensive characterization and analysis of the contact surface and the bulk of aminosiloxane coatings, Analyst 135 (6) (2010) 1375–1381.

[29] E. Lecoq, et al., Plasma polymerization of APTES to elaborate nitrogen containing organosilicon thin films: influence of process parameters and discussion about the growing mechanisms, Plasma Process. Polym. 10 (3) (2013) 250–261.

[30] B. Verheyde, D. Havermans, A. Vanhulsel, Characterization and tribological behaviour of siloxane-based plasma coatings on HNBR rubber, Plasma Process. Polym. 8 (8) (2011) 755–762.

[31] K.H. Kale, S.S. Palaskar, Plasma enhanced chemical vapor deposition of tetraethylorthosilicate and hexamethyldisiloxane on polyester fabrics under pulsed and continuous wave discharge, J. Appl. Polym. Sci. 125 (5) (2012) 3996–4006.

[32] M. Garzia Trulli, et al., Deposition of aminosilane coatings on porous Al2O3 microspheres by means of dielectric barrier discharges, Plasma Process. Polym. 14 (9) (2017) 1600211.

[33] S.C. Larsen, Nanocrystalline zeolites and zeolite Structures: synthesis, characterization, and applications, J. Phys. Chem. C 111 (50) (2007) 18464–18474.

[34] H. Valdés, R.F. Tardón, C.A. Zaror, Role of surface hydroxyl groups of acid-treated natural zeolite on the heterogeneous catalytic ozonation of methylene blue contaminated waters, Chem. Eng. J. 211–212 (2012) 388–395.

[35] J. Rivera-Utrilla, et al., Enhanced oxidation of sodium dodecylbenzenesulfonate aqueous solution using ozonation catalyzed by base treated zeolite, Chem. Eng. J. 180 (2012) 204–209.

[36] C.W. Kwong, et al., Catalytic ozonation of toluene using zeolite and MCM-41 materials, Environ. Sci. Technol. 42 (22) (2008) 8504–8509.

[37] K. Okumura, et al., Quick XAFS studies on the Y-type zeolite supported Au catalysts for CO—O2 reaction, J. Phys. Chem. B 109 (25) (2005) 12380–12386.

[38] J. Lu, et al., Imaging isolated gold atom catalytic sites in zeolite NaY, Angew. Chem. 124 (24) (2012) 5944–5948.

[39] Ji, et al., Enhanced protein digestion through the confinement of nanozeolite-assembled microchip reactors, Anal. Chem. 80 (7) (2008) 2457–2463.

[40] Y. Huang, et al., Zeolite nanoparticle modified microchip reactor for efficient protein digestion, Lab Chip 6 (4) (2006) 534–539.

[41] Y. Pan, et al., Preparation of uniform nano-sized zeolite A crystals in microstructured reactors using manipulated organic template-free synthesis solutions, Chem. Commun. (46) (2009) 7233–7235.

[42] K. Yeung, S. Kwan, W. Lau, Zeolites in microsystems for chemical synthesis and energy generation, Top. Catal. 52 (1–2) (2009) 101–110.

[43] N.C. Pérez, E.E. Miró, J.M. Zamaro, Cu, Ce/mordenite coatings on FeCrAl-alloy corrugated foils employed as catalytic microreactors for CO oxidation, Catal. Today 213 (2013) 183–191.

[44] X. Tan, K. Li, Membrane microreactors for catalytic reactions, J. Appl. Chem. Biotechnol. 88 (10) (2013) 1771–1779.

[45] G. Zhang, et al., Continuous flow ZIF-8/NaA composite membrane microreactor for efficient Knoevenagel condensation, Catal. Commun. 68 (2015) 93–96.

[46] K.B. Yoon, Organization of zeolite microcrystals for production of functional materials, Acc. Chem. Res. 40 (1) (2007) 29–40.

[47] S.Y. Choi, et al., Monolayer assembly of zeolite crystals on glass with fullerene as the covalent linker, J. Am. Chem. Soc. 122 (21) (2000) 5201–5209.

[48] R. Jafari, et al., Stable plasma polymerized acrylic acid coating deposited on polyethylene (PE) films in a low frequency discharge (70 kHz), React. Funct. Polym. 66 (12) (2006) 1757–1765.

[49] Q. Li, D. Creaser, J. Sterte, An investigation of the nucleation/crystallization kinetics of nanosized colloidal faujasite zeolites, Chem. Mater. 14 (3) (2002) 1319–1324.

[50] S.J. Oh, et al., Characteristics of DNA microarrays fabricated on various aminosilane layers, Langmuir 18 (5) (2002) 1764–1769.

[51] E.A. Smith, W. Chen, How to prevent the loss of surface functionality derived from aminosilanes, Langmuir the Acs Journal of Surfaces & Colloids 24 (21) (2008) 12405.

[52] S. Liu, et al., Evaporation-induced self-assembly of gold nanoparticles into a highly organized two-dimensional array, Phys. Chem. Chem. Phys. 4 (24) (2002) 6059.

[53] R.R. Bhat, et al., Controlling the assembly of nanoparticles using surface grafted molecular and macromolecular gradients, Nanotechnology 14 (10) (2003) 1145–1152.

[54] M.C. Daniel, D. Astruc, Gold nanoparticles: assembly, supramolecular chemistry, quantum-size-related properties, and applications toward biology, catalysis, and nanotechnology, Chem. Rev. 35 (16) (2004) 293–346.

[55] S. Bulou, et al., Study of a pulsed post-discharge plasma deposition process of APTES: synthesis of highly organic pp-APTES thin films with NH2 functionalized polysilsesquioxane evidences, Plasma Process. Polym. 16 (4) (2019) 1800177.

[56] T. Shen, et al., Improved adhesion of Ag NPs to the polyethylene terephthalate surface via atmospheric plasma treatment and surface functionalization, Appl. Surf. Sci. 411 (2017) 411–418.

[57] M.M. Hossain, et al., Robust hydrophobic coating on glass surface by an atmospheric-pressure plasma jet for plasma-polymerisation of hexamethyldisiloxane conjugated with (3-aminopropyl) triethoxysilane, Surf. Eng. 35 (5) (2019) 466–475.

[58] J. Kim, et al., Formation, structure, and reactivity of amino-terminated organic films on silicon substrates, J. Colloid Interface Sci. 329 (1) (2009) 114–119.

[59] R.M. Silverstein, G.C. Bassler, Spectrometric identification of organic compounds, J. Chem. Educ. 39 (11) (1962) 546.

[60] S.M. Kanan, W.T.Y. Tze, C.P. Tripp, Method to double the surface concentration and control the orientation of adsorbed (3-aminopropyl)dimethylethoxysilane on silica powders and glass slides, Langmuir 18 (17) (2002) 6623–6627.

[61] R. Sardar, T.B. Heap, S.P. Js, Versatile solid phase synthesis of gold nanoparticle dimers using an asymmetric functionalization approach, J. Am. Chem. Soc. 129 (17) (2007) 5356–5357.

[62] L. Han, et al., Synthesis of carboxylic group functionalized mesoporous silicas (CFMSs) with various structures, J. Mater. Chem. 17 (12) (2007) 1216–1221.

[63] S. Sanchez-Salcedo, et al., Design and preparation of biocompatible zwitterionic hydroxyapatite, J. Mater. Chem. B 1 (11) (2013) 1595–1606.